J Nanostruct Chem (2014) 4:107
DOI 10.1007/s40097-014-0107-0

ORIGINAL

Synthesis and characterization of ZnS-Ag nanoballs and its application in photocatalytic dye degradation under visible light

P. Sivakumar · G. K. Gaurav Kumar · P. Sivakumar · S. Renganathan

Received: 18 March 2014 / Accepted: 3 May 2014 / Published online: 5 June 2014

Abstract ZnS-Ag nanoballs were synthesized using chemical precipitation method at room temperature aided with the capping agent cetyl trimethyl ammonium bromide. The synthesized nanoballs were characterized by UV–Visible spectrophotometer, diffuse reflectance spectroscopy, X-ray diffraction, high resolution scanning electron microscopy, and energy dispersive X-ray. Photocatalytic activity of ZnS and ZnS-Ag nanoballs was evaluated by irradiating the solution of organic dye methylene blue (MB) in presence of visible light. The different parameters affecting degradation, such as dye concentration, catalyst loading and pH, were studied. Reusability of catalyst was evaluated up to three cycles. Kinetics study was done for the degradation of MB by ZnS and ZnS-Ag nanoballs. It was found that ZnS-Ag nanoballs show higher degradation efficiency than ZnS.

Keywords ZnS-Ag nanoballs · Characterization · Visible light · Photocatalytic degradation · Methylene blue · Kinetics

Introduction

Increase in population and expansion of human settlement lead to development of process industries that use large number of organic compounds and dyes. Effluent containing these substances increases the toxicity in aquatic system. Wastewaters generated by these industries are treated by the various established physical, chemical and biological methods like adsorption, chemical precipitation, electro-coagulation, reverse osmosis, chemical coagulation, chlorination, etc. [1]. The complication related with all the above processes is that they do not degrade the pollutant, but only change it from one form to another and simultaneously produces large amount of secondary products [2].

One of the promising methods evolved was advance oxidation process (AOP) where degradation of organic matters can be easily achieved. AOP's with photocatalyst, H_2O_2, UV, O_3, etc., will lead to the production of OH· radical that can degrade pollutants up to the level of H_2O and CO_2. But the drawback of this method is that it leads to high capital and operating cost [3, 4]. The usage of semiconductor photocatalyst in this processs can be a good option. Different photocatalyst such as metal oxides and sulfides (TiO_2, ZnO, SrO_2, CeO_2, Zns, MnS, CdS, CuS, Sb_2S_3) have been tried for photocatalytic degradation of a wide variety of contaminant [5, 6].

From the literature, it is found that ZnS is having remarkable properties among all the metal sulfides. ZnS is one of the first semiconductor discovered and comes in II–VI group compound. The bulk ZnS is having large band gap of 3.7 eV (Hexagonal wurtzite), 3.3–3.7 eV (Cubic sapherite), which is having exceptional stability against oxidation and hydrolysis. It has been comprehensively studied for wide range of applications like light-emitting

Electronic supplementary material The online version of this article (doi:10.1007/s40097-014-0107-0) contains supplementary material, which is available to authorized users.

P. Sivakumar · G. K. Gaurav Kumar · P. Sivakumar · S. Renganathan (✉)
Department of Chemical Engineering, Anna University, Chennai 600 025, Tamil Nadu, India
e-mail: rengsah@rediffmail.com

P. Sivakumar
Department of Petroleum Engineering, JCT College of Engineering and Technology, Coimbatore 641 105, India

diodes, electro-luminescence, chemical sensors, lasers, biosensors, bio-devices, photoconductors and solar cells [7, 8]. On the other hand, ZnS and ZnS doped by noble metals (Cu, Ag, Au, Co) have important environmental applications in wastewater treatment as an effective photocatalyst [9, 10]. There are many works in the field of doping of Zns with Mn, Cu and Ni. Limited works were done in doping of Ag with ZnS because of the difficult in synthesis like co-precipitation [11].

When a noble metal is doped with photocatalyst and irradiated with visible light, the atom utilizes the photon energy ($h\upsilon$) and reduces band gap. This leads the electrons in semiconductor to move from valence band to conduction band that generates charge carriers (electrons and holes) [12, 13]. These holes are responsible for formation of OH· radicals. These holes and OH· radicals produced in process are responsible for degradation. The role of doped noble metal is very much promising, which results in formation and transfer of charge carriers, in the presence of light. Thus on increasing the available surface area of photocatalyst, the degradation efficiency of dyes also increased [14].

Simple and nontoxic method was selected for the synthesis of ZnS and ZnS-Ag nanoballs at room temperature by chemical precipitation. These nanoballs were used to degrade MB dyes that are used in different fields such as biology, chemistry and in other different industries. MB comes under aromatic compound and is heterocyclic in nature (CAS No [61-73-4], $C_{16}H_{18}ClN_3S{\cdot}2H_2O$). This dye is stable and shows harmful effect if swallowed, inhaled or if it comes in contact with skin. It also leads to severe eye irritation and is also reported to act as a mutating agent [15, 16].

The kinetics study was done for the degradation of MB by ZnS and ZnS-Ag nanoballs under visible light radiation. The effect of various parameters like change in dye concentration, effect of photocatalyst loading, effect of solution pH, and reusability of photocatalyst are studied.

Materials and methods

Materials

All chemicals and reagents used were of analytical grade. Zinc acetate, thio-acetamide (TAA) and cetyl trimethyl ammonium bromide (CTAB) were purchased from Fisher Scientific, Mumbai, India. Silver nitrate ($AgNO_3$) HCl, NaOH, glucose and ethanol were obtained from Merck, Mumbai, India. M.B and deionized water were received from SRL, Mumbai, India. The chemicals obtained were in the highest purity and used directly without further purification.

Catalyst preparation

Synthesis of ZnS nanoballs

The synthesis of ZnS nanoballs was achieved by chemical precipitation method at room temperature. Zinc acetate and TAA were taken in 1:2 ratios. An appropriate solution of zinc acetate (0.5 M in 50 mL deionized water) was stirred for 30 min for proper dissolution in deionized water. Similarly TAA solution (1 M in 50 mL deionized water) was prepared and added dropwise to the zinc acetate solution with constant stirring. It was further stirred for another 2 h. The mixture was centrifuged at 10,000 rpm for 10 min. Then, it was washed with absolute ethanol and deionized water several times to remove possible residual impurities. The precipitate was then dried in an oven at 60 °C for 12 h. After grinding, a white powder of ZnS nanoballs was obtained. TAA reacts with water to form hydrogen sulfide. H_2S dissociated into H^+ and S^{2-} ions. Zn^{2+} obtained from Zinc acetate reacts with S^{2-} to give ZnS. This reaction mechanism involved is summarized as follows (1–3).

$$CH_3CSNH_2 + H_2O \rightarrow CH_3CONH_2 + H_2S \quad (1)$$

(TAA).

$$H_2S \rightarrow H^+ + HS^- \rightarrow 2H^+ + S^{2-} \quad (2)$$

(Hydrogen sulfide).

$$Zn^{2+} + S^{2-} \rightarrow ZnS \quad (3)$$

Synthesis of ZnS-Ag nanoballs

ZnS-Ag nanoballs were synthesized by capping ZnS nanoballs with Ag nanoparticles. Initially, silver nanoparticles were synthesized by the following method:

About 3 g of soluble starch was dissolved in 100 mL of deionized water. 5 mL of 300 mM $AgNO_3$ solution was prepared and added in starch solution. The solution was then autoclaved at 15 Psi, 121 °C for 10 min [17].

To the synthesized ZnS, 0.1 M of CTAB was added with uniform stirring. After complete mixing the Ag nanoparticles synthesized in solution was added dropwise (1 mL min^{-1}) with magnetic stirring till a brown color precipitate began to appear on mixing. After addition, the mixture was centrifuged at 10,000 rpm for 10 min. The precipitate obtained was washed and centrifuged several times to remove possible residual impurities. The precipitate was then dried in an oven at 60 °C for 12 h. After grinding, brownish powder of ZnS-doped Ag nanoballs was obtained.

Catalyst characterization

All the samples were prepared by dispersing them in deionized water. The UV–Vis absorption spectra of

prepared colloidal dispersions were recorded using an UV–Vis spectrophotometer (UV) (Perkin Elmer, USA). Band gap was calculated using a diffuse reflectance spectroscopy (DRS) (JASCO V-650, USA). X-ray diffraction (XRD) studies was done using Philips—1710 diffractometer with Cu $K_{\alpha 1}$ (1.54060 Å), Cu $K_{\alpha 2}$ (1.54443 Å) and Cu K_{β} (1.39225 Å) radiation at 40 kV and 30 mA for 2θ values over 10°–80°. Average size of the particle can be given by the following Debye–Scherrer formula (4).

$$L = \frac{0.9\lambda}{\beta \cos\theta} \tag{4}$$

where: L = apparent size of the crystalline domain in Å, β = full width at half maximum of the diffraction peak, λ = source wavelength in Å, Cosθ = half of the peak position 2θ. A FEI Quanta FEG 200 X high resolution scanning electron microscopy (HR-SEM) with energy dispersive X-ray (EDX) was carried out after gold plating of the samples to study the surface morphology of the ZnS-Ag nanoballs.

Photocatalytic degradation

The degradation of MB in the presence of photocatalyst ZnS and ZnS-Ag was studied using a stimulated day light of 300 W, Xe lamp with a 400-nm cutoff filter. Different concentrations of dye solutions were prepared from stock solution (1,000 ppm). 1.5 mL of MB stock solution was taken in 100 mL of distilled water to prepare 15 ppm solution. 100 mg of photocatalyst (ZnS-Ag) was used for photocatalytic degradation study. The evaluation was carried out in visible light to investigate the efficiency of ZnS and ZnS-Ag nanoballs. Magnetic stirrer was used in the reaction, so that the suspension of catalyst remains uniform during the reaction. At regular interval approximately 5 mL of samples was collected and centrifuged to obtain the nanoparticles for the determination of MB degradation. The absorption spectra of MB degraded sample show maximum absorption at $\lambda_{max} = 656$ nm. The percentage degradation was determined from the Eq. (5).

$$D\% = 100 \times \frac{C_0 - C_t}{c_0} = 100 \times \frac{A_0 - A_t}{A_0} \tag{5}$$

where C_0 and C_t are the initial concentration and concentration of dye at time t. A_0 and A_t are initial and final absorbance at time t. D is the degradation efficiency.

Results and discussion

UV analysis

Optical properties of the ZnS nanoballs and Ag were investigated by UV–Visible absorption spectra. It was observed that there were intensive absorptions in the ultraviolet band in the region 350–400 nm, which were the characteristics peak of ZnS nanoballs (378 nm). Ag nanoparticles show characteristic peak at 424 nm.

DRS analysis

DRS was used to calculate band gap for particular substance. The spectrum of ZnS and ZnS-Ag nanoballs is shown in Fig. 1. The chemically synthesized ZnS nanoballs were having band gap of 3.21 eV. The band gap of synthesized ZnS-Ag nanoballs changed to 3.42 eV after doping Ag. This increase in band gap of 0.21 eV can be explained by its quantum confinement effect of the nanocomposite. Rise in band gap occurs due to the increase in size of nanocomposite synthesized. This was confirmed

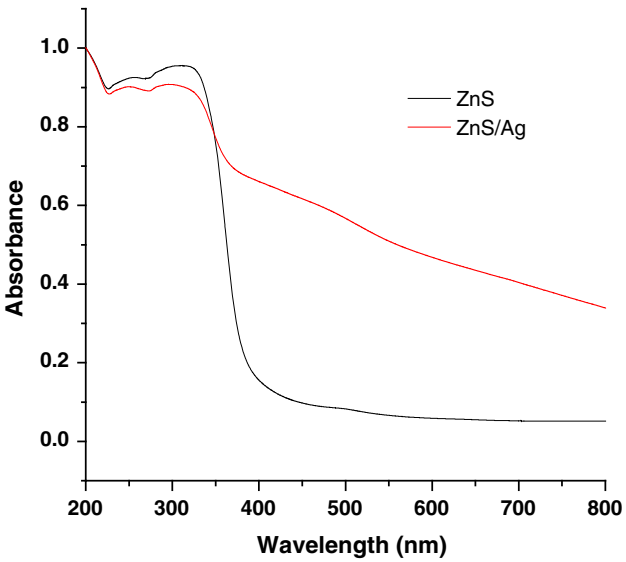

Fig. 1 DRS spectra of ZnS and ZnS-Ag nanoballs

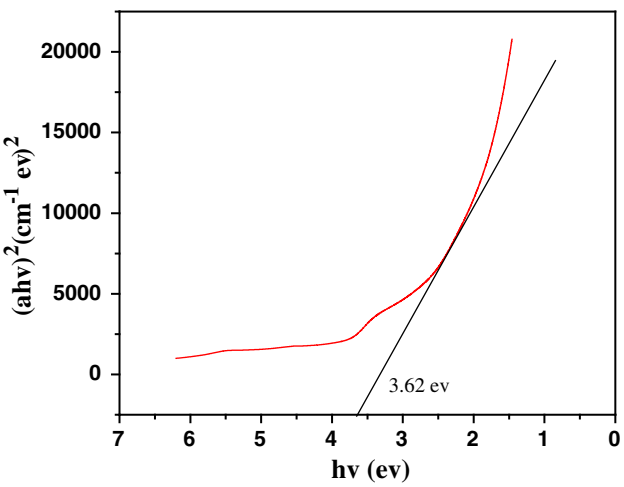

Fig. 2 Tauc Plot of Ag doped ZnS

through XRD and HR-SEM analysis. Tauc plot was used to calculate the more accurate band gap energy by plotting $(\alpha hv)^2$ vs. hv. Here α is absorption co efficient and hv is photon energy. The result shows that band gap energy of Ag doped was 3.62 eV (Fig. 2).

XRD analysis

XRD pattern of ZnS nanoball spectra show various diffraction peaks at 2θ values of 29.33, 48.80 and 57.61 corresponding to the diffraction planes (111), (220) and (311), respectively. The average of crystalline size was obtained as 35 nm using Debye–Scherrer equation.

XRD pattern of ZnS-Ag nanoballs has pointed and more intense peaks than the undoped ZnS nanoballs, which indicates that the synthesized ZnS-Ag nanoballs were crystalline in nature. The spectra show various diffraction peaks at 2θ values of 29.31, 47.93 and 57.30 corresponding to the diffraction planes (111), (220) and (311), respectively. Thus, the average crystalline size of synthesized ZnS-Ag was found to be nearly 41.3 nm.

SEM-EDX analysis

The SEM has been used to characterize the size, shape and morphologies of formed nanoparticles. It shows the uniform spherical shape structure of the ZnS-Ag nanoballs, which were arranged in form of cluster. It reveals that there is large homogeneity at the surface. The particles are nearly spherical ball-like structure. Figure 3 represents the HR-SEM images of the prepared ZnS-Ag nanocomposite. Individual particles are in the range of 45–75 nm, which supports XRD data.

The EDX result of ZnS nanoballs shows the presence of elements Zn and S in the weight percent of 71.79 and 28.21 and atomic percent of about 55.52 and 44.48, respectively. Their weight and atomic percentages were in stoichiometric proportions. The elemental analysis confirms the presence of 100 % ZnS. The EDX of ZnS-Ag nanoballs shows the presence of elements Zn, S and Ag with weight percent of 67.02, 29.99 and 2.99, respectively. Their weight and atomic percentage confirms that Ag was doped on ZnS nanoballs.

Photodegradation of dye using nanophotocatalyst

Photocatalytic degradation of MB was used to evaluate the photocatalytic activities of the synthesized ZnS and ZnS-Ag nanoballs. Figure 4 shows the variation in UV–Vis spectra of MB in the presence of ZnS and ZnS-Ag nanoballs when irradiated for 2 h, respectively. This is because of degradation of MB.

Mechanism of photocatalytic degradation

In the presence of visible light irradiation ($h\upsilon$), ZnS-Ag molecules get excited. The electrons (e^-s) and holes (h^+) are formed. The h^+ present can convert H_2O to OH· and H^+ ion. Free e^-s can reduce molecular O_2 to $O_2^{\cdot-}$. Superoxide radical ($O_2^{\cdot-}$) then reacts with H^+ ion to form HO_2· free radical, which in turn converted to hydrogen peroxide (H_2O_2) and O_2. H_2O_2 in the presence of light leads to synthesis of OH·, simultaneously it can be synthesized with reaction with superoxide radical. OH· is a strong oxidizing agent. The OH· and h^+ produced are very much active and readily degrade the dye. Ag is having specific property of surface Plasmon and can be excited by freely propagating electromagnetic radiation in the visible or UV region. There was increase in particle size after doping Ag with the help of CTAB. The band was shifted to lower energy (red shift) and this leads to increase in band gap [17]. The mechanisms of photocatalytic degradation were shown in the following Eqs. (6–16).

$$\mathrm{ZnS-Ag} + h\upsilon \rightarrow \mathrm{e^-} + \mathrm{h^+} \quad (6)$$

$$\mathrm{H_2O} + \mathrm{h^+} \rightarrow \mathrm{OH\cdot} + \mathrm{H^+} \quad (7)$$

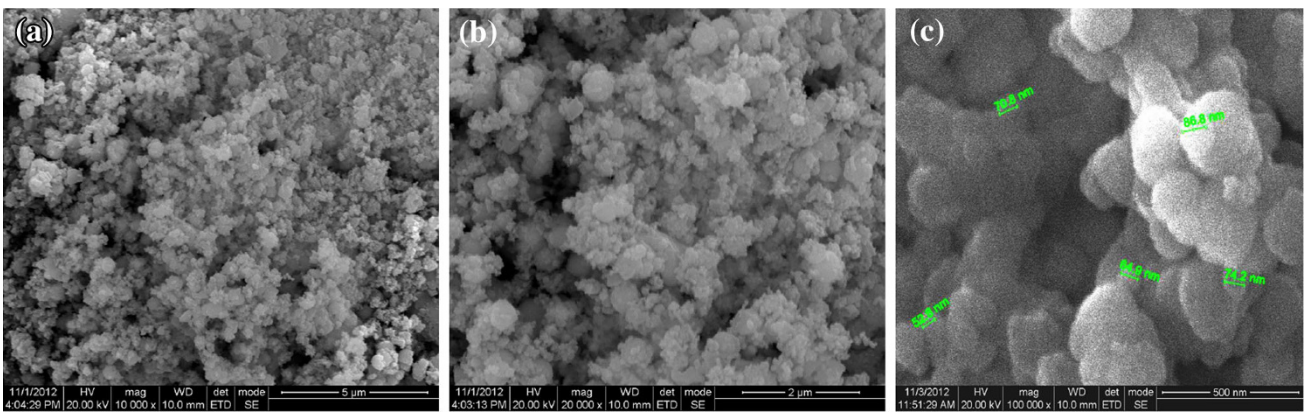

Fig. 3 HR-SEM images of ZnS-Ag nanoballs **a** 5 µm resolution, **b** 2 µm resolution, **c** 500 nm

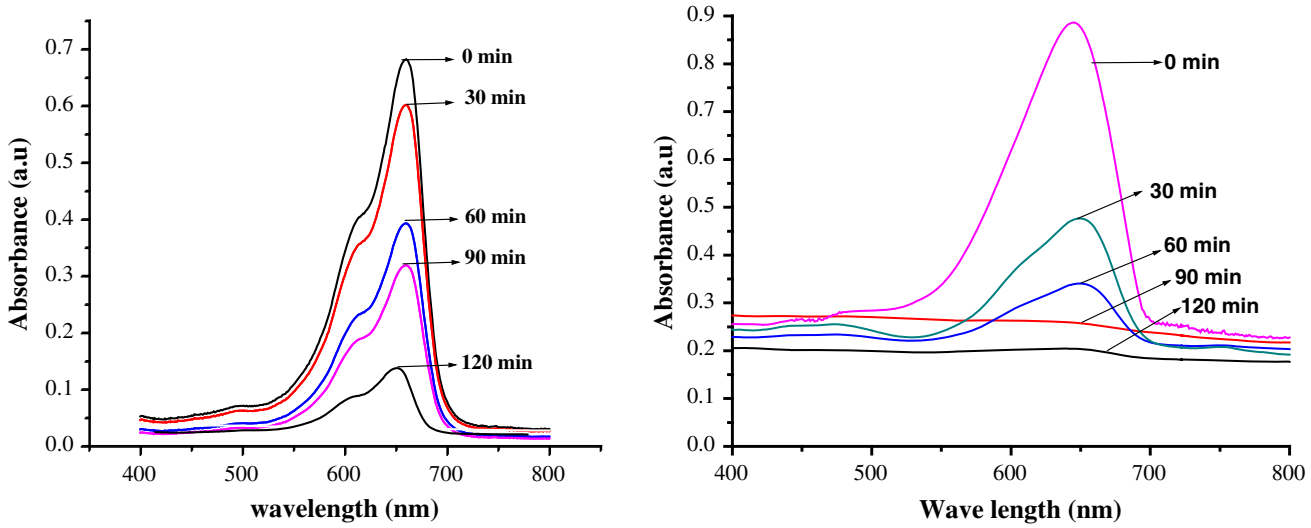

Fig. 4 Variation in UV absorption spectra of methylene blue (15 ppm) in the presence of ZnS and ZnS-Ag photocatalyst

$$O_2 + e^- \rightarrow O_2^{\cdot -} \quad (8)$$

$$O_2^{\bullet -} + H^+ \rightarrow HO_2\cdot \quad (9)$$

$$2\,HO_2\cdot \rightarrow H_2O_2 + O_2 \quad (10)$$

$$HO_2\cdot + OH\cdot \rightarrow H_2O_2 + O_2 \quad (11)$$

$$H_2O_2 + h\upsilon \rightarrow 2OH\cdot \quad (12)$$

$$H_2O_2 + O_2^{\cdot -} \rightarrow OH\cdot + O_2 + O \quad (13)$$

$$H_2O_2 + HO_2\cdot \rightarrow OH\cdot + O_2 + H_2O \quad (14)$$

$$OH\cdot + \text{Dye} \rightarrow \text{Degraded product} \quad (15)$$

$$h^+ + \text{Dye} \rightarrow \text{Degraded product} \quad (16)$$

Degradation kinetics study

Kinetics describes the rate of degradation of MB with respect to time. In general, rate expressions for single component system are typically written in concentration terms as shown in Eq. (17).

$$\frac{d[MB]}{dt} = k[MB]^n \quad (17)$$

where k is the degradation rate constant, $[A]$ is the concentration of the dye, n is the order and t is the time for degradation.

Different kinetic models have been proposed to explain the mechanism of dye degradation [18]. To investigate the mechanism, the concentration data were applied to zero-order, first-order and second-order kinetic models to find the rate of degradation. For zero-order, first-order and second-order mechanisms, (17) can be rewritten as (18), (19) and (20), respectively.

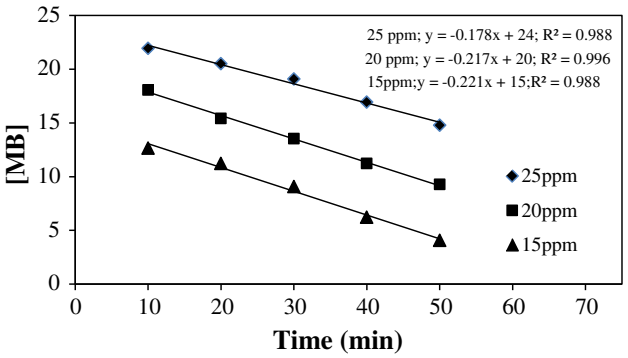

Fig. 5 Kinetic studies for zero order

$$\frac{d[MB]}{dt} = k[MB]^0 \quad (18)$$

$$\frac{d[MB]}{dt} = k[MB]^1 \quad (19)$$

$$\frac{d[MB]}{dt} = k[MB]^2 \quad (20)$$

Taking ln on both side and linearizing the equation into a straight line, $y = mx + C$. The above equations can be written as (21), (22) and (23), respectively.

$$[MB] = kt + [MB]_0 \quad (21)$$

$$\ln[MB] = kt + \ln[MB]_0 \quad (22)$$

$$\frac{1}{[MB]} - \frac{1}{[MB]_0} = kt \quad (23)$$

The integrated rate law equations for zero-, first- and second-order expressions were different functions but all

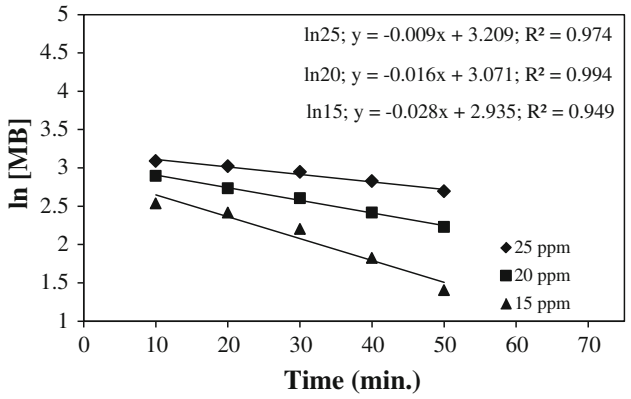

Fig. 6 Kinetic studies for first order

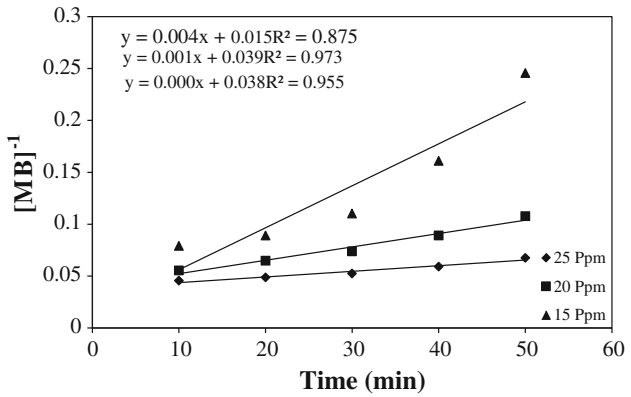

Fig. 7 Kinetic studies for second order

can be shown in the form of a straight line. Kinetic graphs were drawn using the (21), (22) and (23). The kinetic graphs are shown in Figs. 5, 6 and 7.

Figures show the fitting results of zero-, first- and second-order kinetic models based on the experimental degradation data of MB. Thus, it can be confirmed from the graph that degradation follows zero-order kinetic path. Rate constant values were 0.178, 0.217 and 0.221 min^{-1} for different concentrations 25, 20 and 15 ppm, respectively.

The degradation of both doped and undoped nanoparticles was compared. It was observed that ZnS shows approximately 20 % degradation, whereas ZnS-Ag shows 60–70 % degradation in 30 min. Thus, the removal efficiency of MB was nearly 100 % in 2 h. It was further confirmed and explained with kinetics study. ZnS-Ag nanoballs' degradation efficiency is enhanced due to the positive effect of Ag on the photoactivity of ZnS. The degradation of MB may be explained by its ability to inhibit the electron–hole pair recombination and increases the photonic efficiency.

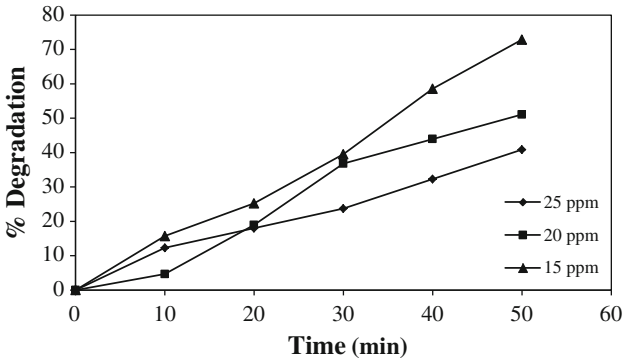

Fig. 8 Effect of change in dye concentration

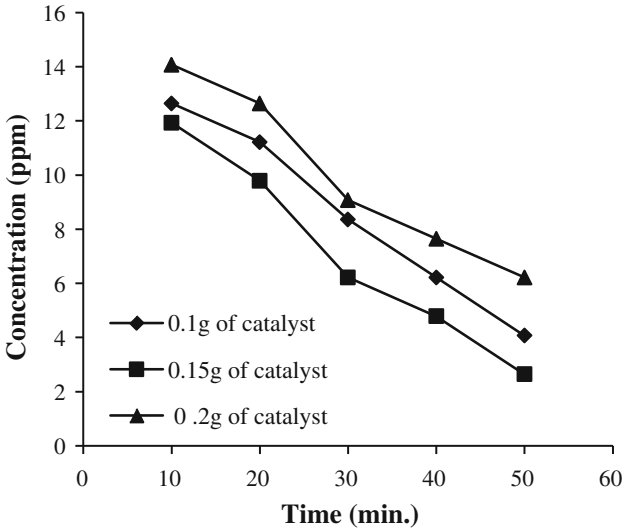

Fig. 9 Effect of photocatalyst concentration

Parameters affecting dye degradation rate

Effect of dye concentration

The effect of varying concentration of MB was studied by keeping the photocatalyst concentration at 100 mg 100 mL^{-1} and degradation study was performed from 0 to 50 min. The degradation of MB decreased as the dye concentration was increased (Fig. 8). This is attributed due to high concentration of dye, which leads to incapability of light to reach the photocatalyst surface. At high dye concentration some amount of light is absorbed by the dye molecule itself. This results in restricted production of OH· and O_2· radical that decreases the possibility of degradation of dye molecule. Degradation is also affected by the structure variation and complexity of dye molecule. Long chain and complex structure of dye hinders the light available for photocatalyst, leading to insignificant photodegradation [19].

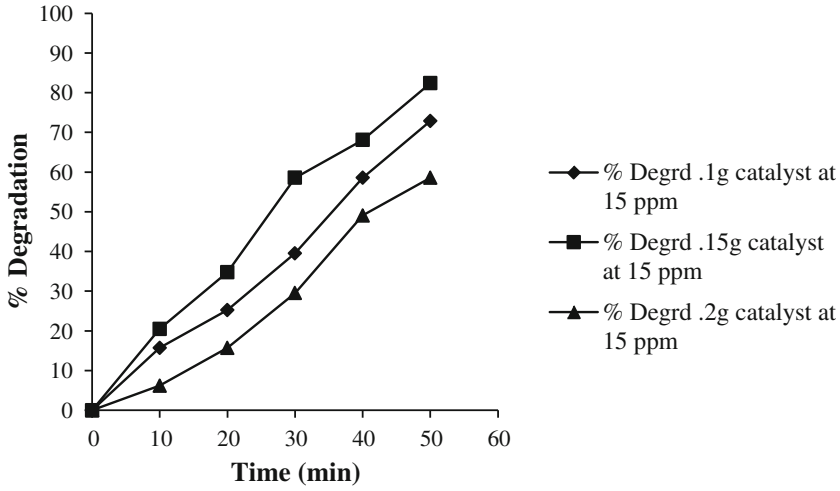

Fig. 10 Rate of degradation with change in photocatalyst concentration

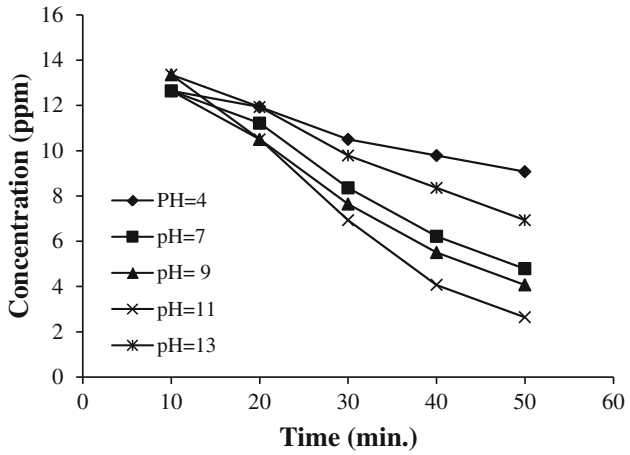

Fig. 11 Effect of pH

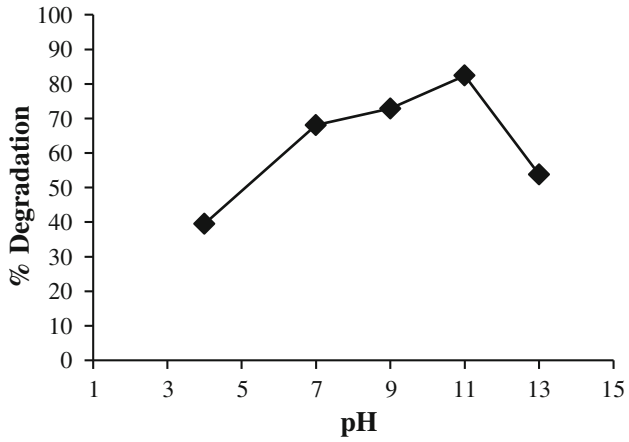

Fig. 12 Rate of degradation with change in pH

Effect of photocatalyst concentration

Photocatalytic degradation of MB was studied by altering the phtocatalyst concentration from 100 to 200 mg keeping the dye concentration constant (15 ppm). Figures 9 and 10 show the degradation of MB in different concentration of photocatalyst. Reaction was performed up to 0–50 min. It was observed that with increase in catalyst concentration up to 150 mg, the degradation rate increases. The degradation rate starts to decrease after 150 mg. This can be explained by the fact that at higher concentration of phtocatalyst (>150 mg), the solution became turbid and the light rays were not able to penetrate and interact with photocatalyst. Thus, less number of photocatalysts was activated. The higher amount of catalyst leads to aggregation and scattering of light, which leads to decrease in degradation efficiency [14].

Effect of pH

pH is one of the important parameters for study of dye degradation. The effect of pH was studied in pH range of 4–13, which was maintained by adding 0.2 M H_2SO_4 and 0.2 M NaOH solution. At low pH, degradation is less, as pH increases degradation increases up to 11, but at pH 13; the degradation decreases drastically as shown in (Figs. 11, 12). At low pH, ZnS nanoballs get dissolved in acidic solution (24).

$$ZnS + 2H^{+}Zn^{+2} + H_2S \quad (24)$$

The photocatalyst has low stability in acidic solution and thus degradation was reduced at lower pH. Photo degradation of catalyst was favored with increasing pH. At higher pH, the formation of OH^{-} radical increases and electrostatic interaction takes place between MB (cationic dye) and nanoparticles. At pH beyond 11, repulsion of OH^{-} ion by the negatively charged photocatalyst surface results in reduced $OH^{\cdot -}$ formation, thus decreasing photodegradation efficiency [20].

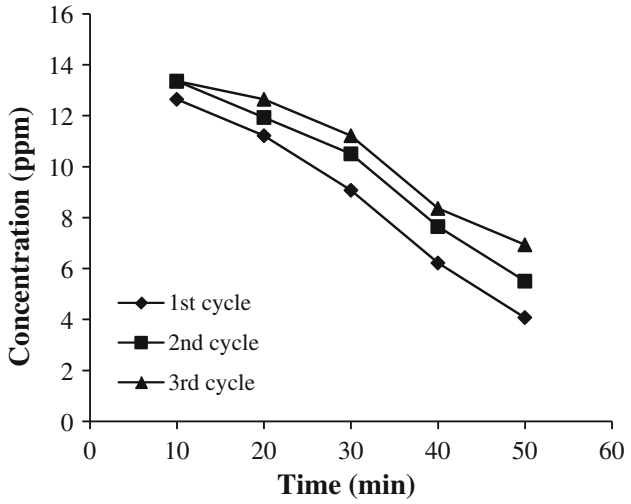

Fig. 13 Effect of reusability of photocatalyst

Reusability of photocatalyst

Reusability of photocatalyst was done by further processing of the degraded sample after the first cycle use of photocatalyst. The degraded dye solution containing catalyst was centrifuged at 10,000 rpm for 10 min. It was washed several times with distilled water and ethanol, which was further dried in hot air oven at 50–60 °C. The dried and powdered photocatalyst was used for next cycles reuse. Nearly 92 % of photocatalyst was recovered after each cycle. It was observed that 50 % of dye degradation was achieved in 50 min, when it was used in the third cycle. It was observed from the graphical result (Fig. 13) that the photocatalyst could be used for three cycles with minimal change in catalyst property and degradability.

Conclusion

ZnS and ZnS-Ag nanoballs were synthesized and characterized successfully, which was used as a photocatalyst for degradation of organic dyes. Kinetic studies were established and it was found that ZnS-Ag was having higher photocatalytic efficiency than ZnS. The different factors influencing the degradation were studied. The intermediates produced in the photodegradation process will be studied in future. It can be concluded that synthesized ZnS-Ag nanocomposites can be used as a favorable photocatalytic degradation material for the organic pollutant.

Acknowledgments We gratefully acknowledge the Council of Scientific and Industrial Research, New Delhi, India for the financial support. P. Sivakumar thanks the Council of Scientific and Industrial Research, Human Resource Development Group (Extra Mural Research Division-1), New Delhi, India, for the award of the Senior Research Fellowship.

References

1. He, T., Maa, H., Zhou, Z., Xu, W., Ren, F., Shi, Z., Wang, J.: Preparation of ZnS fluoropolymer nanocomposites and its photocatalytic degradation of methylene blue. Polym. Degrad. Stab. **94**, 2251–2256 (2009)
2. Khataee, A.R., Pons, M.N., Zahraa, O.: Photocatalytic degradation of three azo dyes using immobilized TiO_2 nanoparticles on glass plates activated by UV light irradiation: influence of dye molecular structure. J. Hazard. Mater. **168**, 451–457 (2009)
3. Chan, S.H.S., Wu, T.Y., Juanb, J.C., Teha, C.Y.: Recent developments of metal oxide semiconductors as photocatalysts in advanced oxidation processes (AOPs) for treatment of dye wastewater. J. Chem. Technol. Biotechnol. **86**, 1130–1158 (2011)
4. Claudia, L., Martinez, T., Kho, R., Mian, O.I., Mehra, R.K.: Efficient photocatalytic degradation of environmental pollutants with mass-produced ZnS nanocrystals. J. Colloid Interface Sci. **240**, 525–532 (2001)
5. Maji, S.K., Dutta, A.K., Srivastava, D.N., Paul, P., Mondal, A., Adhikary, B.: Effective photocatalytic degradation of organic pollutant by ZnS nanocrystals synthesized via thermal decomposition of single-source precursor. Polyhedron **30**, 2493–2498 (2011)
6. Wang, X., Wan, F., Han, K., Chai, C., Jiang, K.: Large-scale synthesis well-dispersed ZnS microspheres and their photoluminescence, photocatalysis properties. Mater. Charact. **59**, 1765–1770 (2008)
7. Xiang, D., Zhu, Y., He, Z., Liu, Z., Luo, J.: A simple one-step synthesis of ZnS nanoparticles via salt-alkali-composited mediated method and investigation on their comparative photocatalytic activity. Mater. Res. Bull. **48**, 188–193 (2013)
8. Fang, X., Zhai, T., Gautam, U.K., Li, L., Wua, L., Bando, Y., Golberg, D.: ZnS nanostructures: from synthesis to applications. Prog. Mater Sci. **56**, 175–287 (2011)
9. Zhang, J., Liu, S., Yu, J., Jaroniec, M.: A simple cation exchange approach to Bi-doped ZnS hollow spheres with enhanced UV and visible-light photocatalytic H_2-production activity. J. Mater. Chem. **21**, 14655–14662 (2011)
10. Zhang, J., Yu, J., Zhang, Y., Li, Q., Gong, J.R.: Visible light photocatalytic H_2-production activity of CuS/ZnS porous nanosheets based on photoinduced interfacial charge transfer. Nano Lett. **11**, 4774–4779 (2011)
11. Qin, D., Yang, G., He, G., Zhang, L., Zhang, Q., Li, L.: The investigation on synthesis and optical properties of ag-doped ZnS nanocrystals by hydrothermal method. Chalcogenide Lett. **9**, 441–446 (2012)
12. Cheng, B., Le, Y., Yu, J.: Preparation and enhanced photocatalytic activity of Ag@TiO_2 core–shell nanocomposite nanowires. J. Hazard. Mater. **177**, 971–977 (2010)
13. Yu, J., Xiong, J., Cheng, B., Liu, S.: Fabrication and characterization of Ag–TiO_2 multiphase nanocomposite thin films with enhanced photocatalytic activity. Appl. Catal. B **60**, 211–221 (2005)
14. Pouretedal, H.R., Eskandari, H., Keshavarza, M.H., Semnanic, A.: Photodegradation of organic dyes using nanoparticles of

cadmium sulfide doped with manganese, nickel and copper as nanophotocatalyst. Acta Chim. Slov. **56**, 353–361 (2009)
15. Pouretedal, H.R., Norozi, A., Keshavarz, M.H., Semnani, A.: Nanoparticles of zinc sulfide doped with manganese, nickel and copper as nanophotocatalyst in the degradation of organic dyes. J. Hazard. Mater. **162**, 674–681 (2009)
16. Borhade, A.V., Tope, D.R., Uphade, B.K.: An efficient photocatalytic degradation of methyl blue dye by using synthesized PbO nanoparticles. E-J. Chem. **9**, 705–715 (2012)
17. Vigneshwaran, N., Nachane, R.P., Balasubramanya, R.H., Varadarajan, P.V.: A novel one-pot 'green' synthesis of stable silver nanoparticles using soluble starch. Carbohydr. Res. **341**, 2012–2018 (2006)
18. Pouretedal, H.R., Keshavarz, M.H.: Study of congo red photodegradation kinetic catalyzed by $Zn_{1-X}Cu_XS$ and $Zn_{1-X}Ni_XS$ nanoparticles. Int. J. Phys. Sci. **6**, 6268–6279 (2011)
19. Shirsath, S.R., Pinjari, D.V., Gogate, P.R., Sonawane, S.H., Pandit, A.B.: Ultrasound assisted synthesis of doped TiO_2 nanoparticles: characterization and comparison of effectiveness for photocatalytic oxidation of dyestuff effluent. Ultrason. Sonochem. **20**, 277–286 (2013)
20. Moghaddam, M.B., Yangjeh, A.H.: Effect of operational parameters on photodegradation of methylene blue on ZnS nanoparticles prepared in presence of an ionic liquid as a highly efficient photocatalyst. J. Iran. Chem. Soc. **8**, 169–175 (2011)